

Parametric Modelling and Experimental Evaluation of Hemispherical Solar Still for Fresh Water Production

R.Jayaprakash^{a*}, T. Arunkumar^a, Sanjay Kumar^b

^aSolar Energy Laboratory, Department of Physics, Sri Ramakrishna Mission Vidyalaya College of Arts and Science, Coimbatore-641020, Tamilnadu, India

^bCentre for Renewable Energy and Environmental Research, P.O. Box – 5, Muzaffarpur - 842001, Bihar, India,
Email: prof.ssinha@gmail.com

* Corresponding author Tel.: 0422 6562371; E-mail address: jprakash_jpr@rediffmail.com

Abstract

Nowadays most of the industrial waste water is contaminated with impurities. The purification of water by the conventional method is costlier as well as, more time and energy consuming. So this work reports that a newly designed solar still with hemispherical top cover for industrial waste desalination purpose. The theoretical and experimental investigation of a hemispherical solar still with flowing water over the cover has been presented. The daily distillate output of the system is almost increased by lowering the temperature of the cover by water flowing over it at a uniform velocity. The fresh water output is presented for a typical day in Sri Ramakrishna Mission Vidyalaya College of Arts and Science, Coimbatore (11° North, 77° East), India. Explicit expressions for the different performance parameters such as water temperature, cover temperature, air temperature, ambient temperature and distillate output have been obtained. The output from the top cover cooling effect of hemispherical solar still has also been compared with the still without cooling method.

Keywords: Desalination; Hemi spherical solar still; Efficiency

Glossary

A	Area (m ²)
C	Specific heat of acrylic cover (J/kg °C)
d	Thickness of the cover (10 ⁻³ m)
g	Acceleration due to gravity(m/s ²)
Gr	Grashof number
h _r	Radiative heat transfer coefficient, (W/m ² °C)
h ₁	Total heat transfer coefficient from water surface to the acrylic cover (W/m ² °C)
h ₂	Total heat transfer from the cover to ambient (W/m ² °C)
h ₃	Heat transfer coefficient comprising convective heat transfer coefficient from absorber plate to water and total heat transfer coefficient from bottom surface to ambient (W/m ² °C)
h ₄	Convective heat transfer coefficient from bottom of the still to atmosphere (W/m ² °C)
I	Solar intensity (W/m ²)
I _d	Diffuse component (W/m ²)
I _b	Beam component (W/m ²)
K	Thermal conductivity (W/m °C)
h _{fg}	Latent heat of vaporization (J/kg)

M	Mass of the water in the basin (kg)
n	Day of the year
Nu	Nusselt number
Pr	Prandlt number
q	Heat transfer flux, ($\text{W}/\text{m}^2 \text{ } ^\circ\text{C}$)
R_b	The ratio between the direct solar radiation received by a horizontal surface, and the direct solar radiation over an inclined surface
t	Time (sec)
T	Temperature ($^\circ\text{C}$)
V	Wind velocity (m/s)

Subscripts

a	Ambient
b	Beam radiation, basin
c	Cover, convection, cooling
d	Diffuse radiation
e	Evaporation
ga	Cover to air
i,j	Dependent variables
s	Surface area
sky	Sky temperature
r	Radiation
w	water

Greek letters

α	Absorbitivity
β	Coefficient of volume expansion of the fluid, slope
θ	Angle
ρ	Density of the acrylic cover, ground surface reflectivity
φ	Latitude
δ	Declination angle
γ	Surface azimuth angle
η	Efficiency
τ	Transmissivity
σ	Stefan-Boltzmann's constant, $\text{W}/\text{m}^2\text{K}^4$

1. Introduction

Fresh water is an immediate need for human life as drinking water purpose. The 97% of available water sources are saline and include harmful bacteria and 2% is frozen in glaciers and polar ice caps. Hence, only 1% of the world's water is usable for drinking and domestic utilities Velmurugan et al. (2009). Ismail (2009) studied the design and performance of a transportable hemispherical solar still. The result showed that, the daily distilled water output from the still ranged from 2.8 l/m².day to 5.7 l/m².day. Normally in solar still, the heat of vaporization is transferred by convection and radiation. However, the radiation and convection losses from the still are relatively small, which is leading to an increase in the cover temperature and reduction in the temperature difference between water in the basin and the cover. This is mainly affecting the rate of vaporization, and productivity. The cover temperature can be reduced by cooling. This can be accomplished by flowing water film over the transparent cover (e.g. glass) (Reali, Modica (2008), Phadatare and Verma (2007), Tiwari et al. (1997), Toure et al. (1999) or flowing water between a double glass cover Suneja and Tiwari (1998), El- Sebail (2000). Suneja and Tiwari (1999) investigated the effect of water flow over the glass cover of a single slope solar still productivity. In their still the intermittent flow of waste hot water in the basin was maintained. The effect of water flow over of a simple solar still was investigated by Lawrance et al. (1990). They conducted numerical simulations that were validated using their own experiments for a typical summer day. Their results shows that the efficiency of the still increases as the water film flow rate increases and is more significant at large heat capacity of water mass in the basin. Abu-Hijleh (1996), Abu-Hijleh and Mousa (1997) theoretically investigated solar still performance with flowing water as a film over the cover of a single-glass solar still. It was reported that with the proper use of film cooling parameters, the still efficiency could be improved by as much as 20% when accounting for evaporation from the film and 6% without considering evaporation.

This study consists of mathematical modeling of a hemispherical solar still with and without cooling effect by water flowing on a cover. Comparative performance analysis was also conducted for experimental study under the climatic conditions of Coimbatore, India.

2. System description

The water storage basin of the still is constructed with a diameter of 0.95 m and a height of 0.10 m using mild steel. The water storage basin is painted with black paint to increase the absorptivity. The water drainage segment of 0.02 m breadth and 0.02 m height is fixed at the inner perimeter of the basin wall. The still is filled with the water to a height of 0.05 m. The top hemispherical cover is made up of transparent acrylic sheet of 3 mm thickness with transmittance 88 %. Hemispherical cover of diameter 0.945 m and height 0.20 m is designed for the still. *The outer box for the still is made of 4 mm thickness wood with the dimension 1.10 m x 1.10 m x 0.25 m. The bottom of the basin is filled with the sawdust of 0.15 m thickness.* The sides of the basin are insulated with the glass wool. This insulation is made to reduce the conduction heat loss through the base and sides of the solar still. The effect of the cooling on the top cover is analyzed by designing a separate segment for collecting the flow water at the top surface of the cover and they are shown in Figs. 1-3.

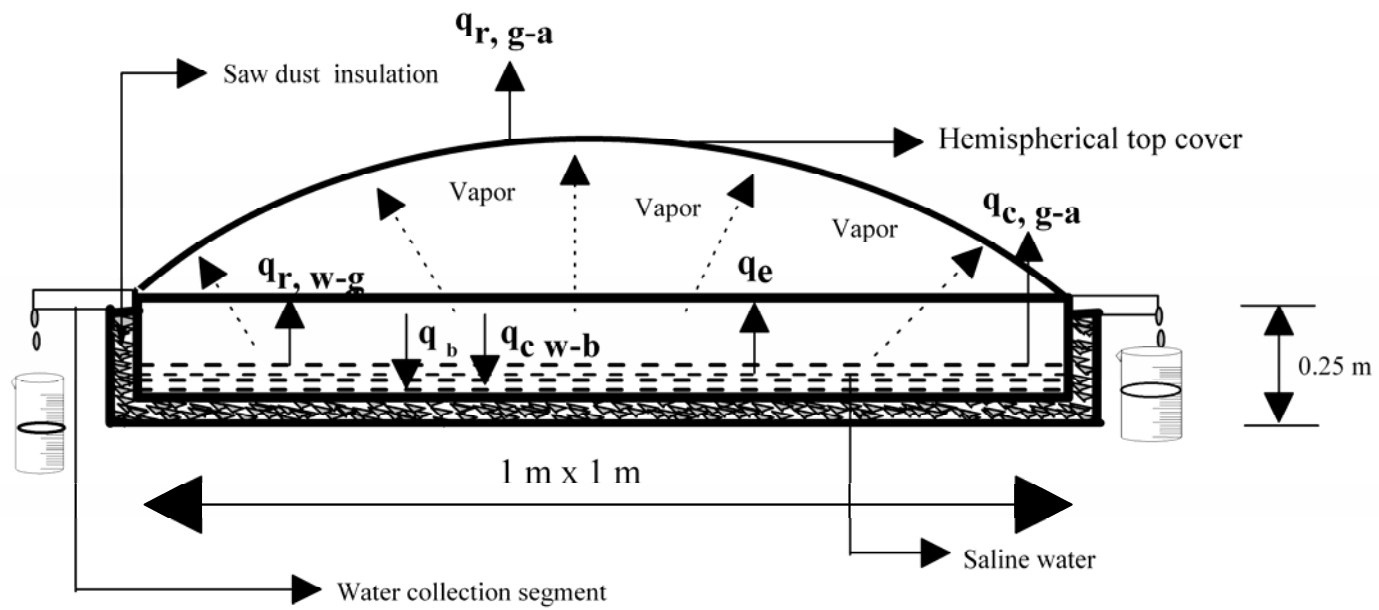


Fig. 1 Cross sectional view of a hemi spherical solar still

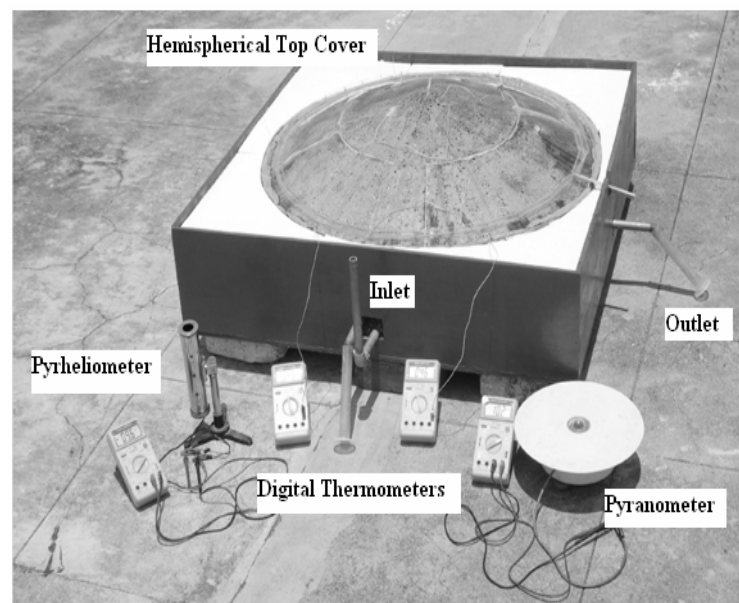


Fig. 2 Experimental solar still

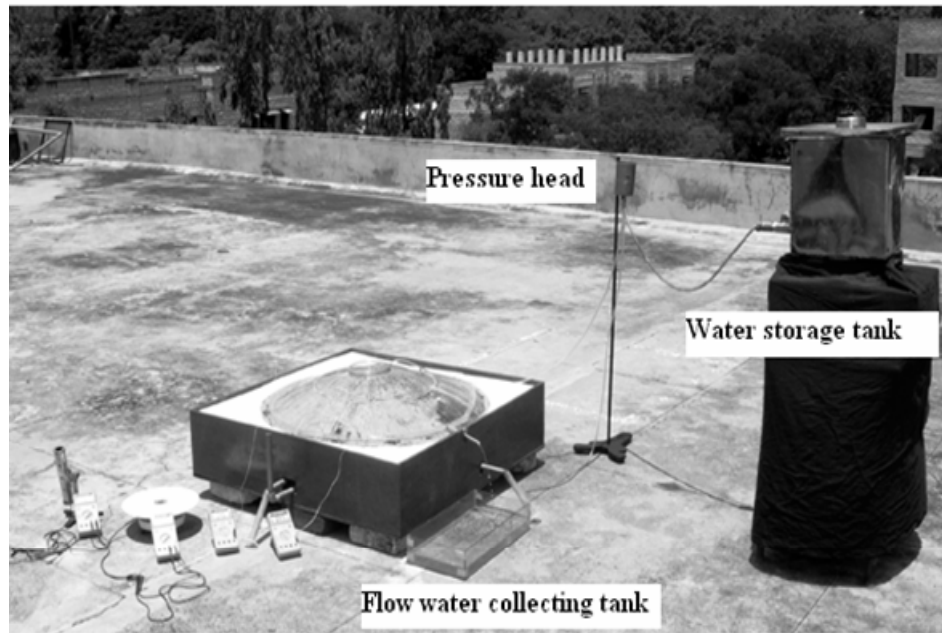


Fig. 3 Solar still with water flowing over the top cover

The solar radiation passed through the hemispherical acrylic top cover, and solar energy was absorbed by the blackened absorber basin. The energy absorbed by the absorber basin was mostly transferred to the water. As a result, water heated and initiated the evaporation. The evaporated water was condensed on the inner surface of the top cover by releasing its latent heat. The condensed water, under gravity, trickled down from the top cover in the distilled water drainage and was finally collected. The temperature of the top cover was an important parameter for the condensation. Generally, wind affected the temperature of the top cover naturally. Here, the idea was cooling the top cover by means of a controlled way. This controlled cooling method was carried by flowing water on the outer surface of the top cover with a constant flow rate.

3. Mathematical Modeling of the System

3.1 Basic Assumption

1. The amount of water lost through evaporation is small compared to the amount of saline water in the basin.
2. There is no leakage of water vapor from the still.
3. The surface area of the hemi spherical top cover is considered.
4. The area of the water surface and the base of the still are considered as equal.
5. The transmittance of the acrylic sheet is not affected by moisture.
6. The wind velocity is constant.
7. All the sides are well insulated.
8. *The energy balance is carried out per unit area of basin water.*

3.2 Simulation procedure

The energy balance equation of the hemispherical solar still is written in the form of finite difference method. A time step of 10 seconds is used. The initial temperature of the still is assumed as ambient temperature. The ambient temperature (T_a) is assumed as constant throughout the day. The daily average radiation is calculated as 11° N latitude (Braun and Mitchell, 1983) which is received over the hemispherical surface. This daily radiation is taken to simulate the performance of the hemispherical solar still.

The energy balance equation for this model is solved by involving initial conditions, boundary conditions and overall losses. The hourly variation of temperature rise in the still is predicted by giving the number of iterations. A flow chart for simulation model is illustrated in Fig. 4.

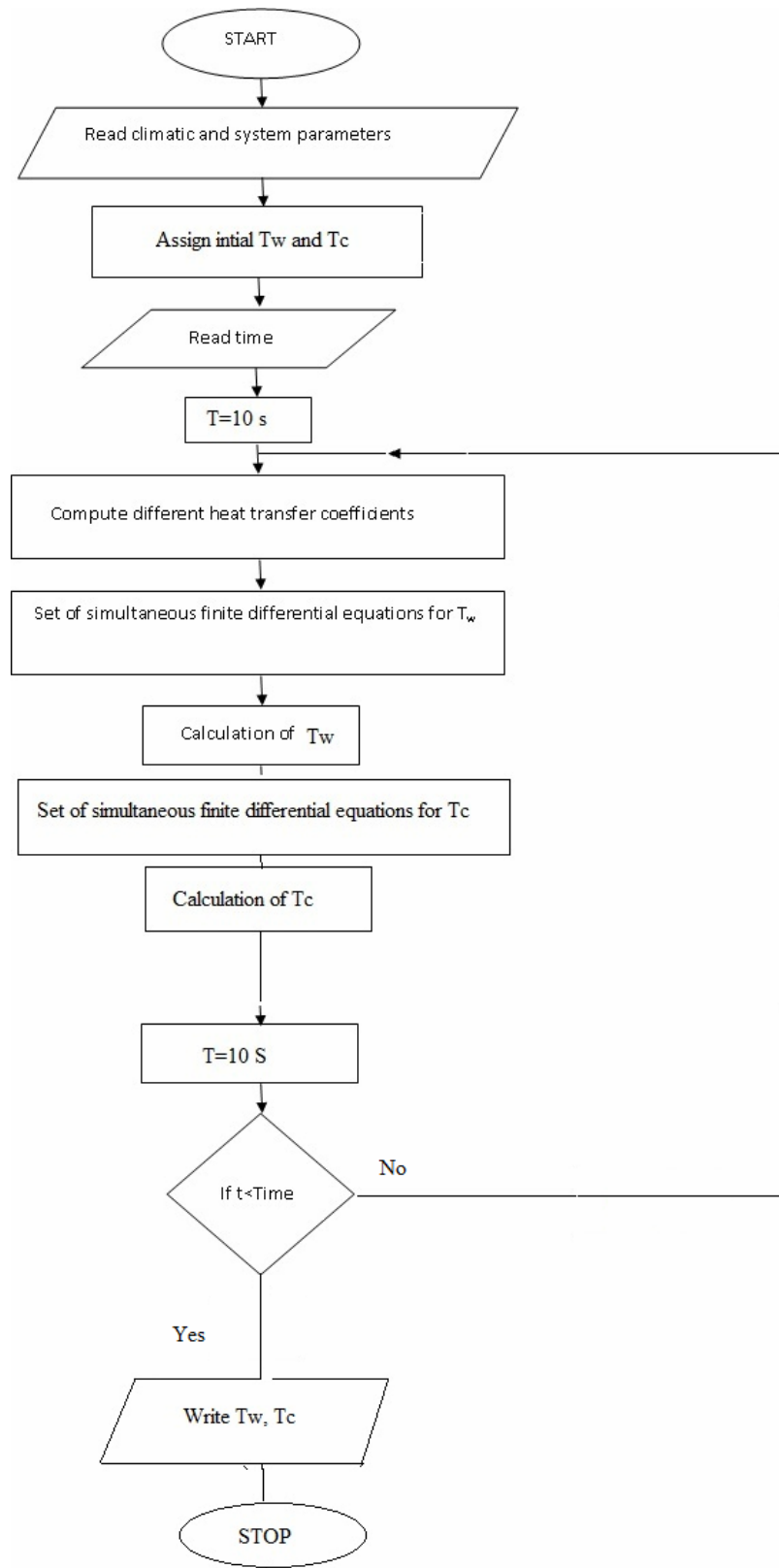


Fig.4 Flow chart of computer methodology

where γ_s is the solar azimuth angle and θ_z is the zenith angle. The solar azimuth angle γ_s is obtained from the expression:

$$\cos \gamma_s = \frac{(\cos \theta_z \sin \phi - \sin \delta)}{\sin \theta_z \cos \phi} \quad (3)$$

For horizontal surfaces, the angle of incidence is the zenith angle of the sun (that is, at 0° or 90° when the sun is above the horizon), hence, $\beta = 0$ and (1) becomes

$$\cos \theta_z = \sin \delta \sin \phi + \cos \delta \cos \phi \cos \omega \quad (4)$$

When $\theta_z = 90^\circ$, $\omega = \omega_s$ and (4) becomes

$$\omega_s = \cos^{-1}(-\tan \delta \tan \phi) \quad (5)$$

where ω_s is the sunset hour angle in degrees. Solar declination angle can be approximated by a sinusoidal variation as:

$$\delta = 23.45^\circ \sin \left(360^\circ \frac{284 + n}{365} \right), \quad (6)$$

Where n is the day number of the year, starting with 1 for January 1st i.e. $1 \leq n \leq 365$. The geometric ratio (factor) is ratio of beam radiation on the tilted surface to beam radiation on the horizontal surface given as:

$$R_b = \frac{\cos \theta}{\cos \theta_z} \quad (7)$$

The hourly diffuse and global solar radiation is respectively computed as:

$$I_d = \frac{\pi \bar{H}_d}{24} \frac{\cos \omega - \cos \omega_s}{\left(\sin \omega_s - \frac{\pi \omega_s \cos \omega_s}{180} \right)} \quad (8)$$

$$I_{t,\beta} = \frac{\pi \bar{H}}{24} \frac{\cos \omega - \cos \omega_s (a + b \cos \omega)}{\left(\sin \omega_s - \frac{\pi \omega_s \cos \omega_s}{180} \right)} \quad (9)$$

And hourly beam radiation is:

$$I_b = I_{t,\beta} - I_d \quad (10)$$

where $I_{t,\beta}$, I_b , and I_d respectively is the hourly global, beam and diffuse solar radiation on a horizontal surface. The anisotropy index, A_i is given as:

$$A_i = \frac{I_b}{I_0} \quad (11)$$

where I_0 is the hourly extraterrestrial radiation on a horizontal surface defined as:

$$I_0 = I_{sc} \left(1 + 0.033 \cos \frac{360n}{365} \right) [\sin \delta \sin \phi + \cos \delta \cos \phi \cos \omega] \quad (12)$$

The horizon brightening f is given as:

$$f = \sqrt{\frac{I_b}{I_{t,\beta}}} \quad (13)$$

The global solar irradiance on the spherical surface:

$$I_{t,\beta} = R_b (I_b + I_d A_i) + I_d (1 - A_i) \left(\frac{1 + \cos \beta}{2} \right) \left(1 + f \sin^3 \left(\frac{\beta}{2} \right) \right) + (I_b + I_d) \rho_g \left(\frac{1 - \cos \beta}{2} \right) \quad (14)$$

where β is the inclination (tilt) of the surface ($^\circ$) and ρ_g is the ground reflectance or albedo (%). The calculated values are shown in Table 1.

Table 1: Derived parameters

Serial.	β	$\cos \theta$	θ	$\cos \theta_z$	θ_z	$\cos \gamma_s$	γ_s	R_b	A_i	f
No										
1	0	0.99985	0.99	0.97748	12.18	-1	-180	1.02	0.0016	0.48

The energy balance equation is written in the form of the partial differential equation for top cover as

$$M_c C_c \left(\frac{\partial T_c}{\partial t} \right) = [A_s \alpha_c I_{t,\beta} + q_w (T_w - T_c) - h_{1g} A_s (T_c - T_a)] \quad (15)$$

Where T_w , T_c and T_a are the temperature of the water, cover and air, M_c and C_c is the mass and the specific heat of the cover, respectively

Where

$$M_c = A_c d_c \rho$$

$$q_w = q_r + q_c + q_e$$

$$q_c = 0.8831(T_w - T_g)[(T_w - T_g) + \left[\frac{(p_w - p_g)(T_w + 273)}{0.265 - p_w} \right]^{0.33}]$$

$$q_e = 1.92 \times 10^{-3} (P_w - P_g) L_w [(T_w - T_g) + \left[\frac{(P_w - P_g)(T_w + 273)}{0.265 - P_w} \right]^{0.33}]$$

$$q_r = 0.9\sigma \left[(T_w + 273)^4 - (T_g + 273)^4 \right],$$

$$T_{sky} = (T_{air} - 10)$$

$$q_{sky} = 0.9\sigma \left[(T_w + 273)^4 + (T_a + 273)^4 \right]$$

The above equation can be written in the form of finite difference form for simulation with initial boundary conditions. The energy balance equation in the form of finite difference equation for the top cover is given by,

$$T_{c(i+1)} = T_{ij} + \left(\frac{\Delta t}{M_c C_c} \right) \left\{ [A_s \alpha_c I_{t,\beta}] + [q_w (T_w - T_c)] - [h_{1g} A_s (T_c - T_a)] \right\} \quad (16)$$

Δt is the time difference in seconds.

The initial condition of the equation for top cover in solar still is given by

$$T_c \big|_{initial} = T \big|_{amb}$$

and the boundary conditions is given by

$$T_c \big|_{x=x1} = T \big|_{amb}$$

The energy balance equation is written in the form of partial differential equation for top cover with cooling as

$$M_c C_c \left(\frac{\partial T_c}{\partial t} \right) = [A_s \alpha_c I_{t,\beta} \big|_{x=0} + q_w (T_w - T_c) - h_{1g} A_s (T_c - T_a)] - R_E \quad (17)$$

The energy balance equation in the form of finite difference equation for the top cover cooling is given by,

$$T_{cc(i+1)} = T_{ij} + \left(\frac{\Delta t}{M_c C_c} \right) \left[A_s \alpha_c I_{t,\beta} \Big|_{x=0} \right] + [q_w (T_w - T_c)] - [h_{1g} A_s (T_c - T_a)] - \frac{\Delta t}{M_c C_c} R_E \quad (18)$$

Where

$$R_E = \dot{m} C_w (T_{out} - T_{in})$$

The initial condition of the equation for top cover cooling in solar still is given by

$$T_{cc} \Big|_{initial} = T \Big|_{amb}$$

The energy balance equation is written in the form of the partial differential equation for water in the hemispherical solar still as

$$M_w C_w \left(\frac{\partial T_w}{\partial t} \right) = A_w \alpha_w \left[I_{t,\beta} \Big|_{x=x_1} \tau_c - I_{t,\beta} \Big|_{x=x_l} \tau_w \right] - [h_{1w} (T_w - T_c) - h_3 A_w (T_{basin} - T_w)] \quad (19)$$

Where T_w , T_c are the temperature of the water, cover, M_w and C_w is the mass and the specific heat of the water, respectively. Convective heat transfer coefficient from basin linear to water termed as h_3 . 'I' is the solar intensity radiation.

Where

$$M_w = A_s d_w \rho$$

$$q_w = q_r + q_c + q_e$$

$$h_3 = \frac{C k_f}{x_1} \left[\frac{x_1^3 \rho_f^2 g \beta \Delta T}{\mu_f^2} \cdot \frac{C_{pf} \mu_f}{k_f} \right]^{-1}$$

Where

The above partial differential equation for water in the solar still can be written in the form of finite difference form for simulation with initial boundary conditions. The energy balance equation in the form of finite difference equation for water is given by

$$T_{w(i+1)} = T_{ij} + \left(\frac{\Delta t}{M_w C_w} \right) A_w \alpha_w (I_{t,\beta} \Big|_{x=c} \tau_c - I_{t,\beta} \Big|_{x=L} \tau_w) - \left(\frac{\Delta t}{M_w C_w} \right) [h_{1w} (T_w - T_c) - h_3 (T_{basin} - T_w)] \quad (20)$$

The initial conditions of equations for water in solar still is given by

$$T_w \Big|_{initial} = T \Big|_{amb}$$

$$T_{basin} \Big|_{initial} = T \Big|_{water}$$

And the boundary conditions is given by

$$T_w \Big|_{x=x_1} = T_w \Big|_{x=x_L}$$

The values of saturation vapor pressure are predicted under the expression, which is suggested by Brooker. et al., (1978).

$$P = \frac{6893.03 \exp(54.63 - 12301.69/T')}{T' - 5.17 \ln T'} \quad (21)$$

$$T' = (1.8T + 491.69)$$

The Latent heat can be expressed as (Tiwari and Tiwari, 2006)

$$h_{fg} = 2.4935 \times 10^6 \left[1 - 9.4779 \times 10^{-4} \times T_i + 1.3132 \times 10^{-7} \times T_i^2 - 4.7974 \times 10^{-10} \times T_i^3 \right] \quad (22)$$

$$T_{av} = \frac{(T_w + T_c)}{2}$$

4. Water analytical results

Water quality analysis was tested at the Tamilnadu Agricultural University's, Soil Science and Agricultural Chemistry Department in Coimbatore. The results thus obtained are presented in Table.2. Two different water samples were tested. Two parameters, pH and Electrical Conductive (dSm^{-1}) were measured before and after these samples became desalinated. Before desalination, the level of electrical conductivity in the water was around 1dSm^{-1} which is quite high. However, it decreased to 0.10dSm^{-1} after desalination. The pH is the most important parameter as far as water quality in an area is concerned. The optimum pH required varies from one water sample to another as well as on the nature of the construction materials used in the water distribution system. It is usually in the range of 6.5 to 8.

Table 2: Tested water quality results

Sample no.	pH		Conductivity(dSm^{-1})	
	Before desalination	After desalination	Before desalination	After desalination
Sample. A-B	7.60	7.32	1 (High saline)	0.10 (Very low saline)

5. Cost Analysis

The cost estimation for various components used in the fabrication of hemispherical solar still is given in Table. 3. The total cost of the fabricated hemispherical acrylic solar still including labor charge was approximately \$161.31.

Table 3: Cost estimation for the components of the fabricated hemispherical solar still

Component	Cost(\$)
Acrylic sheet	47.55
Steel basin	45.29
Outer box	33.97
Pipe and fittings	22.64
Black paint and primers	11.32
Saw dust (Insulation)	4.53
Total cost	\$165.31

6. Results and Discussion

The parameters used in the simulation are given in Table 4. The still temperature is recorded using K-type thermocouples and digital temperature indicators. The solar radiation intensity on the horizontal surface, along with its beam component is recorded with the help of precision Pyranometer respectively (accuracy $\pm 3\%$). The daily productivity is obtained as a summation of day and night productivity.

Table 4: Simulation parameters (El- Sebai, 2000)

Parameters	Symbol	Value
Transmissivity of cover	τ_c	88%
Convective heat transfer coefficient	h_c	10 (W/m ² °C)
Radiative heat transfer coefficient	h_r	5.4 (W/m ² °C)
Specific heat capacity of cover	C_c	1.67 J/kg °C
Specific heat capacity of water	C_w	4190 J/kg °C
Emissivity of cover	ε_c	0.98
Wind velocity	V	1 m/s
Density of water	P	989 kg/m ³
Latent heat of vaporization	h_{fg}	2372000 (J/kg)
Declination angle	Δ	23.18°
Latitude	Φ	11°
Surface azimuth angle	γ_s	68.11°

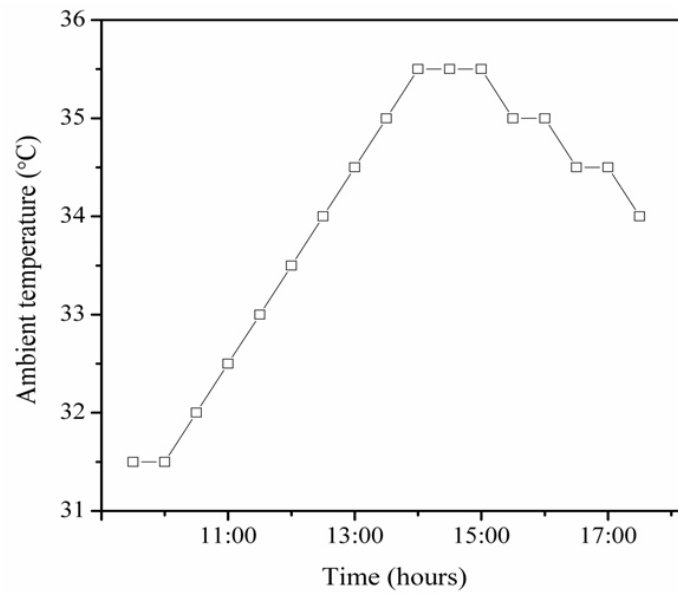


Fig. 6 Ambient temperature on a typical day of Coimbatore, India

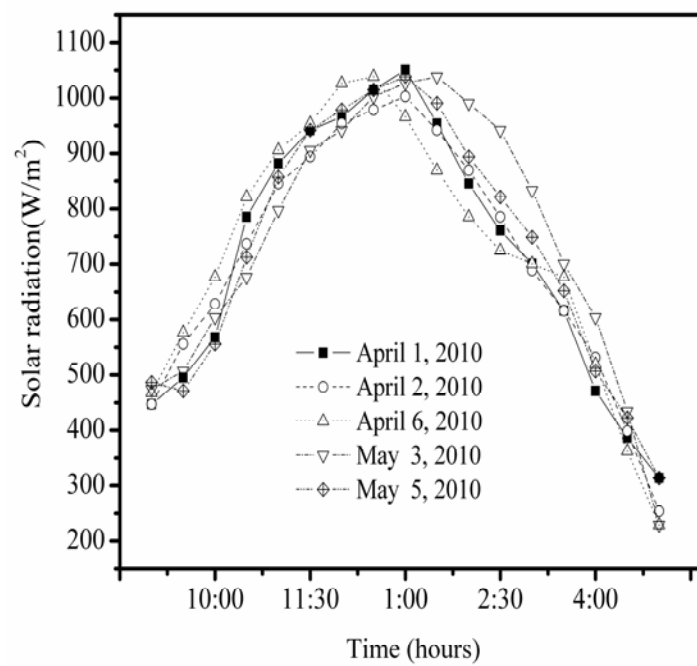


Fig. 7 Solar radiation with respect to time for without cooling experiment

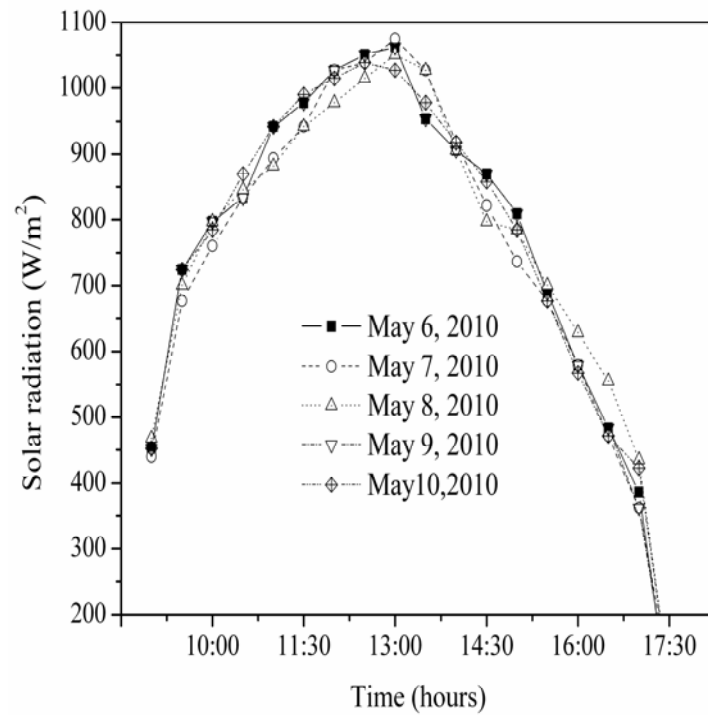


Fig. 8 Solar radiation with respect to time for with cooling experiment

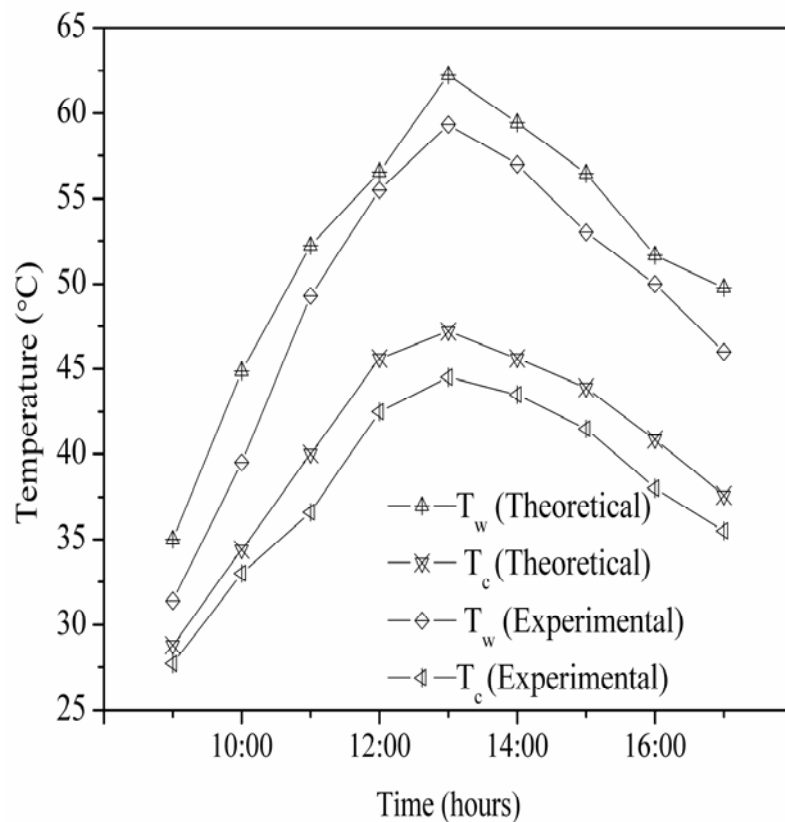


Fig. 9 Comparison between the theoretical and experimental values of water temperature (T_w) and cover temperature (T_c) of the hemispherical solar still (Without top cover cooling)

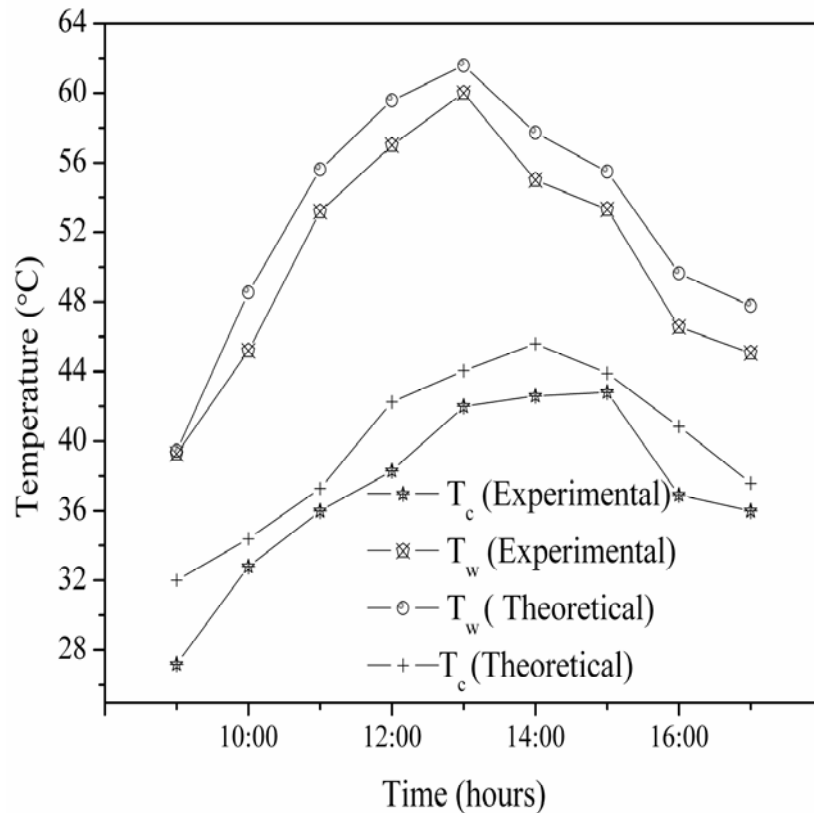


Fig. 10 Comparison between the theoretical and experimental values of water temperature (T_w) and cover temperature (T_c) of the hemispherical solar still (With top cover cooling)

The variation of ambient temperature with respect to time is shown in Fig. 6. The variations of solar radiation intensity for with and without cooling experiments are shown in Figs.7-8. The radiation received during the experimental study for the comparison is considered as clear sky days. The average radiation received in both the experiment is 759 W/m^2 . Fig. 9 shows the variation for water and cover temperatures (without cooling top cover) inside the still in both the experimental and theoretical study. The maximum rise in water temperature is observed as 62.2°C for experimental and 64.24°C for theoretical study. Similarly, the maximum cover temperature is observed as 44.5°C for experimental and 46.5°C for theoretical study. Fig. 10 shows the variation for water and cover temperatures with cooling effect of top cover of the still in both the experimental and theoretical study. The maximum rise in water temperature is observed as 61.58°C for theoretical and 60°C for experimental study. Similarly, the maximum cover temperature is observed as 42.8°C for experimental and 45.59°C for theoretical study. These results revealed that the experimental and theoretical results are obtained as same trend.

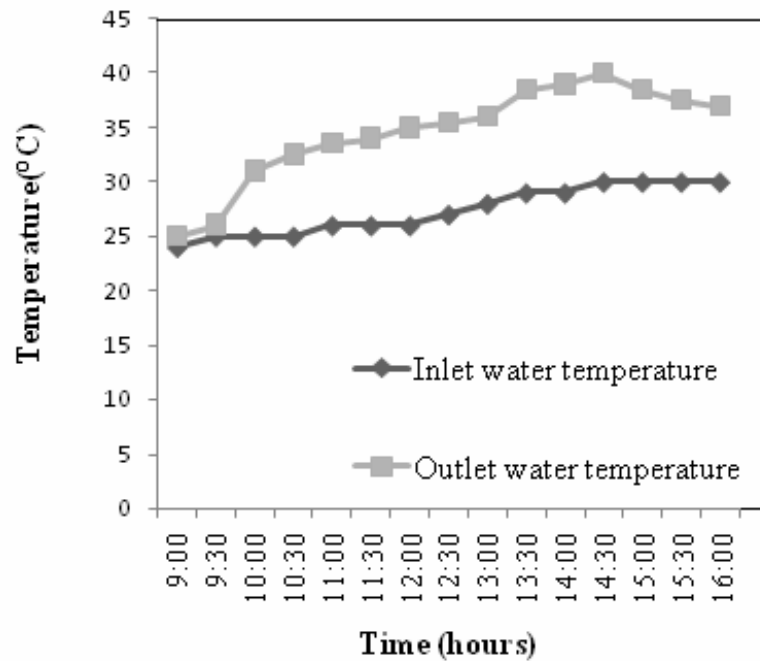


Fig. 11 Cooling water temperature with respect to time

The outlet temperature of cooling water load tank is shown in Fig. 11. A small variation in the initial water temperature is observed due to ambient temperature and the solar radiation falling on it, which causes the variation in inlet temperature. The inlet temperature is in the range of 24°C-30°C. The heat extraction from the top cover due to cooling is observed certainly from the rise in cooling water temperature. The variation of cooling water temperature is in the range of 25°C-40°C. It indicates a rise in outlet water temperature during cooling process.

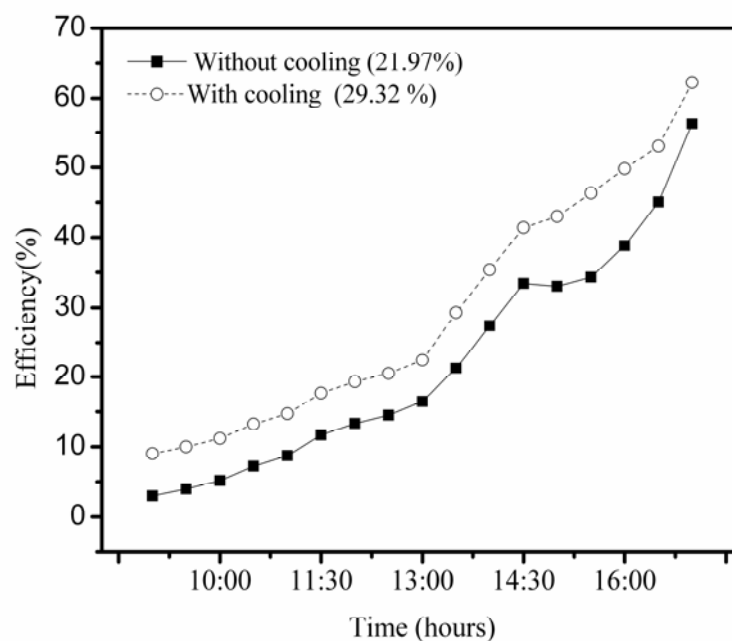


Fig. 12 Efficiency with respect to time

Fig. 12 shows the still's efficiency as a function of time for typical day in April 2010. An improvement in efficiency of 29.32% is achieved for the cooling effect of hemispherical solar still and conventional still achieved as 21.97%. The efficiency of the still is calculated using the formula

$$\eta_i = \frac{M \times L}{A \times I_{t,\beta} \times t} \times 100 \quad (23)$$

Where, 'M' is the mass of the distillate output, 'I' represent the solar radiation, 'A' is the absorber area and 't' is the time interval.

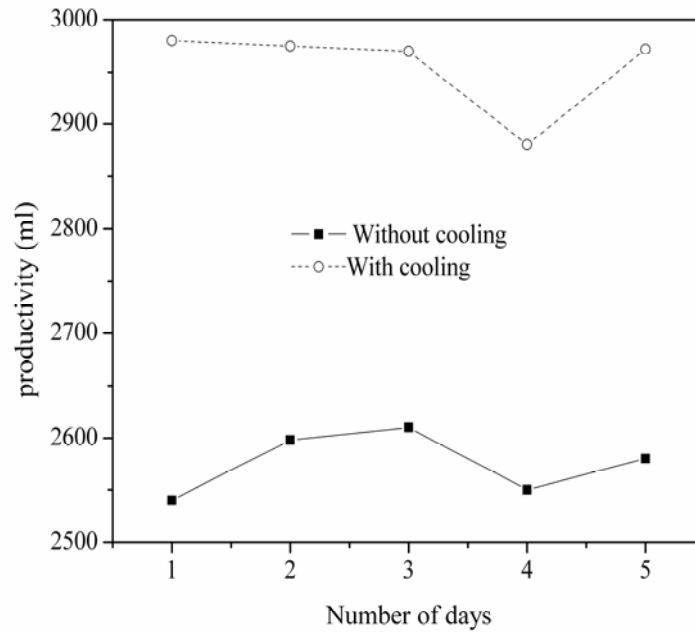


Fig. 13 Still productivity with respect to time

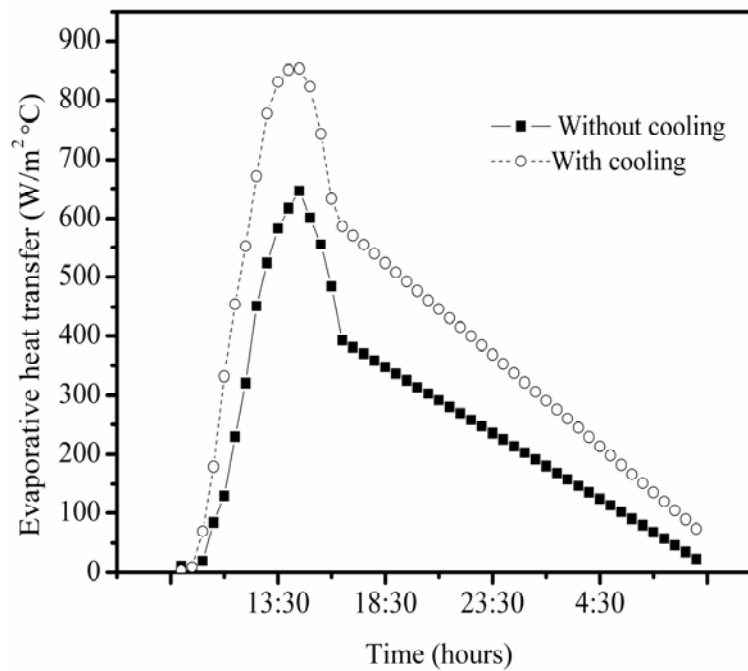


Fig. 14 Evaporative heat transfer with respect to time

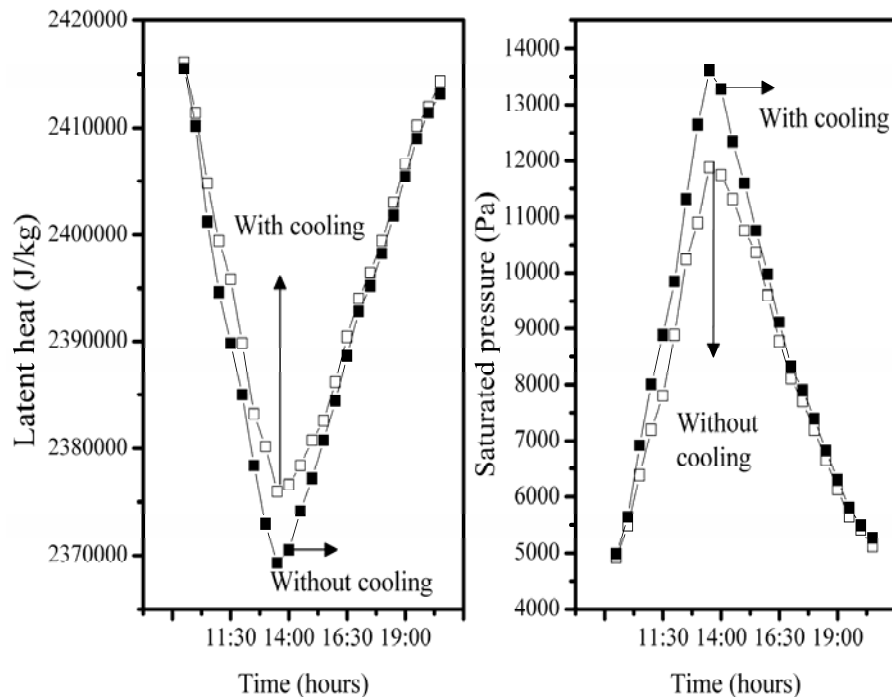


Fig. 15 Hourly variation of latent heat and saturation pressure for with and without cooling study

Results for the output of the still are shown in Fig. 13. The driving force of the solar distillation technique is the difference between temperature of water in the still basin and temperature of the cover ($T_w - T_c$). The existence of such temperature difference ensures the continuation of the distillation process. Clearly, the hemispherical solar still with top cover water cooling is superior to the conventional solar still. This increase of output is justified in Fig. 14. The productivity of the hemispherical solar still is moderately improved by cooling the top cover. The variation of distilled yield is in the range of 2540 ml/m²-day to 2610 ml/m²-day for without water flow and 2970 ml/m²-day to 2980 ml/m²-day for with flow of cold water on the top cover. The productivity is increased from 2598 ml/m²-day to 2980 ml/m²-day for a fixed flow rate of 0.065 ml of water fed during the study. Normally temperature difference between the top cover and ambient temperature plays a major part for condensing the water droplets at the top cover of the still. The surface area of the hemispherical solar still is more when compared with single slope solar still. So the hemispherical top cover is contacted with air in high rate and so it improves the condensate of more droplets in the top cover. The yield rate is much improved for this type of still when compared to single slope conventional solar still (Tris et al, 1998). A shadow effect creates a small amount of shadow to fall over the water surface during in the morning time as well as in the evening time. This type of drawbacks is fully rectified by reducing the height of the basin as well as hemispherical shape top cover. Thus the shadow effect does not affect the rise in water temperature.

The evaporative heat transfer coefficient is the major heat loss and is greater than the other two modes together such as radiative heat transfer coefficient (Q_{rw}) and convective heat transfer coefficient (Q_{cw}). This indicates the strong dependence of evaporative heat transfer coefficient on the operating water temperature (T_w). The effect of water flow over the condensing cover on the evaporative heat transfer coefficient is shown in Fig. 13 for a 0.05 m water depth. The evaporative heat transfer is in the range between 2.9 W/m² to 854 W/m² for top cover cooling method and 11.52 W/m² to 645 W/m² for conventional without cooling performance of the still.

Fig. 14 shows the variation of latent heat and saturated pressure with respect to time. It shows that the latent heat starts to decrease and saturated pressure starts to increase with time. It indicates that the latent heat of evaporation is decreased at increasing temperature. But the saturation pressure reaches maximum value when water collection is more and tends to decrease when water collection decreases.

7. Conclusion

A hemispherical solar still has been fabricated and tested under with and without top cover cooling methods. The still has been theoretically modeled. The production rate depends on water, top cover and atmospheric temperatures. The driving force of the solar distillation technique is the difference between temperature of water in the still basin and temperature of the cover ($T_w - T_c$). The daily production of the still alone is 2598 ml/m²-day, and the production improved up to 2980 ml/m²-day with top cover cooling effect.

References

- Abu-Hijleh, B. A.K., 1996. Enhanced solar still performance using water film cooling of the glass cover, *Desalination*.107, 235-44.
- Abu-Hijleh, B. A.K., Mousa, H. A., 1997. Water film cooling over the glass cover of a still including evaporation effects. *Energy*.22, 43-8.
- Basel I. Ismail., 2009.Design and performance of a transportable hemispherical solar still. *Renewable Energy*. 34,145-50.
- Braun, J.E., Michell J.C., 1983. Solar geometry for fixed and tracking surfaces, *Solar Energy*. 31, 439-44.
- Brooker D.B., Bakker-Arkma F.W., Hall C.W, *Drying Cereal Grain*. AVI West Port, U.S.A, 1978.
- Cooper,P.I., 1969.The absorption of solar radiation in solar stills, *solar Energy*. 12,333-46
- El- Sebail, A.A., 2000.Effect of wind speed on some designs of solar stills. *Energy Convers. Manage*. 41,523-38.
- Lawrence, S.A., Gupta, S.P., Tiwari, G.N., 1990.Effect of heat capacity on the performance of solar still with water flow over the glass cover. *Energy Convers. Manage*. 30, 277-85.
- Malik M.A.S. *Solar distillation*, 1st edition: Pergamon press; 1982.
- Phadatar, M.K., Verma, S.K., 2007. Influence of water depth an internal heat and mass transfer in a plastic solar still. *Desalination*. 217, 267-75.
- Real, M., Modica, G., 2008. Solar stills made with tubes for sea water desalting. *Desalination*. 220,626-32.
- Suneja, S., Tiwari, G.N., 1998. Optimization of number of effects for higher yield from inverted absorber solar still using the Runge-Kutta method, *Desalination*.120, 197-09.
- Suneja, S., Tiwari, G.N., 1999.Effect of water flow on internal solar distillation. *Energy Convers. Manage*. 40, 509-18.
- Tiris, C., Tiris, M., Erdalli, Y.,Sohmen, M., 1998. Experimental studies on a solar still coupled with a flat plate collector and a single basin still. *Energy Convers. Manage*.39,853-56.
- Tiwari ,A.K., Tiwari ,G.N., 2006. Effect of water depths on heat and mass transfer in a passive solar still: In summer climatic condition, *Desalination* 195, 78-4.
- Tiwari, G.N., Kupfernann A., Aggarwal S., 1997. Convective mass transfer in a double condensing chamber solar still. *Desalination*.114, 153-64.
- Toure ,S., Salami, H., Meukam, P., 1999. Theoretical and experimental studies of a solar still type suitable for alcoholic distillation, *Renew Energ*. 16,732-42.
- Velmurugan, V., Gopalakrishnan., Raghu ,M., Srithar, R K., 2009. Single basin solar still with fin for enhancing productivity. *Energy Convers. Manage*. 49, 2602-608.